

Modeling of Arrhythmogenic Automaticity Induced by Stretch in Rat Atrial Myocytes

Jae Boum Youm¹, Chae Hun Leem², Yin Hua Zhang³, Nari Kim¹, Jin Han¹, and Yung E. Earm⁴

¹National Research Laboratory for Mitochondrial Signaling, Department of Physiology and Biophysics, College of Medicine, Inje University, Busan 614-735, ²Department of Physiology and the Institute for Calcium Research, University of Ulsan College of Medicine, Seoul 138-736, Korea, ³Department of Cardiovascular Medicine, University of Oxford, Level 6, West Wing, John Radcliffe Hospital, Headley Way, Headington, Oxford OX3 9DU, UK, ⁴Department of Physiology and National Research Laboratory for Cellular Signalling, Seoul National University College of Medicine, Seoul 110-799, Korea

Since first discovered in chick skeletal muscles, stretch-activated channels (SACs) have been proposed as a probable mechano-transducer of the mechanical stimulus at the cellular level. Channel properties have been studied in both the single-channel and the whole-cell level. There is growing evidence to indicate that major stretch-induced changes in electrical activity are mediated by activation of these channels. We aimed to investigate the mechanism of stretch-induced automaticity by exploiting a recent mathematical model of rat atrial myocytes which had been established to reproduce cellular activities such as the action potential, Ca^{2+} transients, and contractile force. The incorporation of SACs into the mathematical model, based on experimental results, successfully reproduced the repetitive firing of spontaneous action potentials by stretch. The induced automaticity was composed of two phases. The early phase was driven by increased background conductance of voltage-gated Na^+ channel, whereas the later phase was driven by the reverse-mode operation of $\text{Na}^+/\text{Ca}^{2+}$ exchange current secondary to the accumulation of Na^+ and Ca^{2+} through SACs. These results of simulation successfully demonstrate how the SACs can induce automaticity in a single atrial myocyte which may act as a focus to initiate and maintain atrial fibrillation in concert with other arrhythmogenic changes in the heart.

Key Words: Stretch, Automaticity, Atrial fibrillation, Modeling

INTRODUCTION

Atrial fibrillation (AF) is the most common cardiac arrhythmia which leads to several episodes of irregular heart-beat which lasts from minutes to weeks. Patients with AF usually have accompanying hemodynamic or mechanical disorders which elevate intra-atrial pressure or volume overload. Clinical evidence shows that atrial dilatation by increased intra-atrial pressure may predispose to AF. The left atrial enlargement has been proposed as one of risk factors predisposing to nonrheumatic atrial fibrillation (Vaziri et al, 1994). The incidence of AF in older adults also suggests that left atrial size is an important risk factor of AF (Psaty et al, 1997). In isolated rabbit atria, it was demonstrated that raising intra-atrial pressure could induce AF (Franz and Bode, 2003). Therefore, the atrial stretch has been proposed to play an important role in the development of AF.

Myocardial stretch has been found to modulate electrical activity of the heart in various ways, including generation of after-depolarization (Lab, 1978; Franz et al, 1989; Hansen, 1993), depolarization of the resting potential

(Boland and Troquet, 1980; Franz et al, 1992), and alteration of the action potential duration (Dean and Lab, 1989; Franz et al, 1989; Taggart, 1996). Increasing stretch induces also repetitive firing of spontaneous action potentials (APs) without electrical stimulation in papillary muscle of Rhesus monkey, showing the AF-inducible potential of stretch (Kaufmann and Theophile, 1967). The proarrhythmic effects of stretch have been demonstrated in rabbit atrial tissue, where increasing intra-atrial pressure leads to premature depolarizations and runs of non-sustained atrial fibrillation (Bode et al, 2000).

There is a lot of evidence to show that the stretch-activated channels (SACs) are involved in the generation of stretch-induced changes in electrical activity (Bustamante et al, 1991; Craelius, 1993; Hoyer et al, 1994; Kiseleva et al, 2000; Zhang et al, 2000), leading to the idea that SACs may act as a trigger of cardiac arrhythmias. The stretch-induced AF was successfully inhibited by venom of the tarantula *Grammostola spatulata* which is a blocker of SACs, thus favoring the idea that SACs contribute to initiation and maintenance of AF (Bode et al, 2001). The possibility of inducing automaticity by SACs was demonstrated in isolated rat atrial myocytes by incorporation of a stretch-acti-

Corresponding to: Jae Boum Youm, Department of Physiology and Biophysics, College of Medicine, Inje University, 633-165, Gaegum-dong, Busanjin-gu, Busan 614-735, Korea. (Tel) 82-51-890-6426, (Fax) 82-51-894-5714, (E-mail) youmjb@inje.ac.kr, jaeboum@gmail.com

ABBREVIATIONS: SACs, stretch-activated channels; AF, atrial fibrillation; APs, action potentials; SR, sarcoplasmic reticulum; TTX, tetrodotoxin; RyRs, ryanodine receptors.

vated conductance (Wagner et al, 2004). However, there is a limitation of their study in that they did not fully investigate how SACs generate automaticity in rat atrial myocytes. Moreover, the technical difficulty in stretching single myocyte along its longitudinal axis on conducting whole-cell patch clamp without disrupting a gigaseal has been an obstacle to fully investigate the mechanism of AF-generation by stretch.

Recent progress in the mathematical cell-models has encouraged us to reproduce and analyze the role of SACs in inducing AF. Previously, we simulated the effect of stretch on the electrical activity and Ca^{2+} transients of rat atrial myocytes, and investigated which cation species contribute to the stretch-induced changes in electrical activity and Ca^{2+} transients by exploiting a modified Kyoto model (Matsuoka et al, 2003; Sarai et al, 2003) to fit experimental data from rat atrial myocytes (Youm et al, 2006). Based on our previous experimental findings (Zhang et al, 2000), we began this study by reproducing the automaticity of rat atrial myocytes after incorporation of SACs into the mathematical model. We then explored which cellular components and processes are involved in the initiation and/or maintenance of automaticity.

METHODS

General description of mathematical model

The mathematical model used in this study is based mostly on the Kyoto model (Matsuoka et al, 2003; Sarai et al, 2003). The Kyoto model can simulate the myocardial activities including APs, sarcoplasmic reticulum (SR) Ca^{2+} dynamics, and cell contraction of guinea-pig heart. The advantages of the Kyoto model over previous mathematical models such as Oxsoft and Luo-Rudy model have previously been described (Youm et al, 2006). We had to carry out some species-specific modifications to the Kyoto model to simulate our experimental findings in rat atrial myocytes. Furthermore, the ionic currents through the inward rectifier K^+ channel (I_{K1}) and depolarization-activated outward K^+ channel ($I_{K,out}$) were modified to fit the voltage-clamp data of rat atrial myocytes. The maximal con-

Table 1. Parameter details

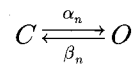
Cell geometry:	
Cell volume:	$V_i=4,046 \mu\text{m}^3$
SR release site:	$V_{rel}=0.02 V_i \mu\text{m}^3$
SR uptake site:	$V_{up}=0.05 V_i \mu\text{m}^3$
Membrane capacitance:	$C_m=50 \text{pF}$
Ionic concentrations used:	
$[\text{K}^+]_i$:	140 mM
$[\text{Na}^+]_i$:	5.4 mM
$[\text{Ca}^{2+}]_i$:	3.5 nM
$[\text{K}^+]_o$:	5.4 mM
$[\text{Na}^+]_o$:	140 mM
$[\text{Ca}^{2+}]_o$:	1.8 mM
Parameters adjusted (see Matsuoka et al, 2003):	
P_{Na} :	1044
P_{CaL} :	11.52
P_{bNSC} :	0.066
$P_{\text{I(Ca)}}$:	0
N for I_{KATP} :	0

ductance of other ion channels was additionally modified to fit the voltage-clamp recordings from rat atrial myocytes. The volume of the cell and ionic concentrations were also adjusted. Finally, the SACs were incorporated into the mathematical model to simulate the stretch-induced effects as previously described (Youm et al, 2006). Details of all parameters and definition of symbols are summarized in Table 1 and 2, respectively.

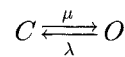
Model formulations for the inward rectifier K^+ current (I_{K1})

Mathematical modelling of I_{K1} is basically based on the Kyoto model, however, some modifications were also made to the model to fit experimental data from rat atrial myocytes as follows.

State C (closed) reversibly goes into state O (open),



State O rapidly goes into state B (blocked).



$$I_{K1}=43.2 \cdot (V-E_K) \cdot ([\text{K}^+]_o/5.4)^{0.62} \cdot n \cdot f_O \quad (1)$$

$$E_K=-86.7([\text{K}^+]_i=140 \text{ mM}, [\text{K}^+]_o=5.4 \text{ mM}) \quad (2)$$

$$\alpha_n=1.0/(8000 \cdot \exp((V-E_K-97)/8.5)+7 \cdot \exp((V-E_K-97)/300)) \quad (3)$$

Table 2. Definition of symbols

Inward rectifier K^+ channel:

I_{K1} : inward rectifier K^+ current, pA

C: closed state

O: open state

B: blocked state

n: activation gate

f_B : fraction of block

f_O : fraction of open

α_n and β_n : opening and closing rate constants, respectively, ms^{-1}

μ : rate constant of block, ms^{-1}

λ : rate constant of unblock, ms^{-1}

Depolarization-activated outward channel:

$I_{K,out}$: depolarization-activated outward K^+ current, pA

$I_{K,fast}$: fast component of depolarization-activated outward K^+ current, pA

$I_{K,slow}$: slow component of depolarization-activated outward K^+ current, pA

m, h: activation and inactivation gate, respectively

α_m and β_m : opening and closing rate constants, respectively, of activation gate, ms^{-1}

α_h and β_h : opening and closing rate constants, respectively, of inactivation gate, ms^{-1}

Stretch-activated channel (SAC)

I_{SAC} : stretch-activated current, pA

$I_{SAC(X)}$: ion X component of I_{SAC} , pA

$P_{SAC(X)}$: convert factor of SAC for ion X, pA mM^{-1}

X_{CF} : constant field for ion X, mM

F: Faraday constant, 96.4867 C mmol^{-1}

R: gas constant, 8.3143 C $\text{mV K}^{-1} \text{mmol}^{-1}$

T: absolute temperature, 298.15 K

V: membrane potential, mV

E_X : equilibrium potential for ion X, mV

$$\beta_n = 1.0 / (0.00014 \cdot \exp((V - E_K - 97) / (-9.1)) + 0.2 \cdot \exp((V - E_K - 97) / (-500))) \quad (4)$$

$$\mu = 12.75 \cdot \exp(0.035 \cdot (V - E_K - 10)) / (1 + \exp(0.015 \cdot (V - E_K - 140))) \quad (5)$$

$$\lambda = 3 \cdot \exp(-0.048 \cdot (V - E_K - 10)) \cdot (1 + \exp(0.064 \cdot (V - E_K - 38))) / (1 + \exp(0.03 \cdot (V - E_K - 70))) \quad (6)$$

$$f_B = \mu / (\mu + \lambda) \quad (7)$$

$$f_O = \lambda / (\mu + \lambda) \quad (8)$$

Model formulations for the depolarization-activated outward K^+ current ($I_{K,out}$)

The outward K^+ currents in rat atrial myocytes could best be described by the sum of two exponential components, which are termed $I_{K,fast}$ and $I_{K,slow}$ to denote the fast and slow components of current decay, respectively (Boyle and Nerbonne, 1992). All the rate constants and maximal conductance were adjusted to fit our experimental results on rat atrial myocytes as follows.

$$I_{K,out} = I_{K,fast} + I_{K,slow} \quad (9)$$

$$I_{K,fast} = I_{K,fast} K + I_{K,fast} Na \quad (10)$$

$$I_{K,fast} K = 2.9 \cdot m \cdot h \cdot K_{CF} \quad (11)$$

$$I_{K,fast} Na = 0.26 \cdot m \cdot h \cdot Na_{CF} \quad (12)$$

$$\alpha_m(I_{K,fast}) = 1 / (1.4 \cdot \exp(V / (-14,241)) + 0.35 \cdot \exp(V / (-15))) \quad (13)$$

$$\beta_m(I_{K,fast}) = 1 / (22.7 \cdot \exp(V / 37.9) + 1,775 \cdot \exp(V / 8.4)) \quad (14)$$

$$\alpha_h(I_{K,fast}) = 1 / (2.5 \cdot \exp(V / 3.2) + 2,195 \cdot \exp(V / 23.6)) \quad (15)$$

$$\beta_h(I_{K,fast}) = 1 / (40.4 \cdot \exp(V / (-76,022)) + 0.29 \cdot \exp(V / (-5.4))) \quad (16)$$

$$I_{K,slow} = I_{K,slow} K + I_{K,slow} Na \quad (17)$$

$$I_{K,slow} K = 1.8 \cdot m \cdot h \cdot K_{CF} \quad (18)$$

$$I_{K,slow} Na = 0.16 \cdot m \cdot h \cdot Na_{CF} \quad (19)$$

$$\alpha_m(I_{K,slow}) = 1 / (0.0002 \cdot \exp(V / (-7.2)) + 1.37 \cdot \exp(V / (-47.8))) \quad (20)$$

$$\beta_m(I_{K,slow}) = 1 / (1,346 \cdot \exp(V / 16.0) + 1,600 \cdot \exp(V / 11.3)) \quad (21)$$

$$\alpha_h(I_{K,slow}) = 1 / (6,613 \cdot \exp(V / 135,222) + 143,392 \cdot \exp(V / 12.1)) \quad (22)$$

$$\beta_h(I_{K,slow}) = 1 / (4,801 \cdot \exp(V / (-125)) + 119 \cdot \exp(V / (-10.3))) \quad (23)$$

Model formulations for the stretch-activated currents (I_{SAC})

The I_{SAC} can be calculated as follows, based on our results on rat atrial myocytes (Zhang et al, 2000; Youm, 2006).

$$I_{SAC} = I_{SAC(Na)} + I_{SAC(K)} + I_{SAC(Ca)} \quad (24)$$

$$I_{SAC(Na)} = P_{SAC(Na)} \cdot Na_{CF} \quad (25)$$

$$I_{SAC(K)} = 1.32 \cdot P_{SAC(Na)} \cdot K_{CF} \quad (26)$$

$$I_{SAC(Ca)} = 0.7 \cdot P_{SAC(Na)} \cdot Ca_{CF} \quad (27)$$

$$P_{SAC(Na)} = 0.55 \quad (28)$$

The value of SAC conductance ($13.6 \mu S / \mu F$) used in the present study corresponds to that activated by 9%-stretch of cells in longitudinal direction. The percentile value of change in cell length by stretch (ΔL) is calculated by equation (29), where $L_{stretch}$ and $L_{original}$ are the cell length during stretch and before stretch, respectively.

$$\Delta L = (L_{stretch} - L_{original}) / L_{original} \times 100 \quad (29)$$

Constant field equations

$$K_{CF} = \frac{F \cdot V}{R \cdot T} \frac{[K^-]_i - [K^+]_o \cdot \exp\left(\frac{-F \cdot V}{R \cdot T}\right)}{1 - \exp\left(\frac{-F \cdot V}{R \cdot T}\right)} \quad (30)$$

$$Na_{CF} = \frac{F \cdot V}{R \cdot T} \frac{[Na^+]_i - [Na^+]_o \cdot \exp\left(\frac{-F \cdot V}{R \cdot T}\right)}{1 - \exp\left(\frac{-F \cdot V}{R \cdot T}\right)} \quad (31)$$

$$Ca_{CF} = \frac{2 \cdot F \cdot V}{R \cdot T} \frac{[Ca^{2+}]_i - [Ca^{2+}]_o \cdot \exp\left(\frac{-2 \cdot F \cdot V}{R \cdot T}\right)}{1 - \exp\left(\frac{-2 \cdot F \cdot V}{R \cdot T}\right)} \quad (32)$$

RESULTS

Simulation of stretch-induced automaticity of rat atrial myocytes

It was previously demonstrated that the increasing stretch eventually results in repetitive firing of spontaneous APs without electrical stimulus in papillary muscle of Rhesus monkey (Kaufmann and Theophile, 1967). We tested whether our mathematical model of rat atrial myocytes could reproduce the observation that the incorporation of a stretch-activated conductance into the rat atrial myocytes could induce automaticity. As shown in Fig. 1A, the activation of SACs without electrical pacing induced the repetitive firing of APs which is composed of early and delayed phases. During the activation of SACs, the resting membrane potential was depolarized as much as 8.0 mV. The repetitive firing was relatively regular in both phases, and the frequency was higher in the early phase compared with that of delayed phase (2.8 Hz vs 1.2 Hz). The release of SACs activation abolished the repetitive firing of APs, leaving only very small amplitude of membrane depolarizations in a short period. The activation of SACs also induced the change in the contractile force (Fig. 1B) and intracellular Ca^{2+} concentration (Fig. 1C). The activation of SACs triggered the early and delayed phases of repetitive Ca^{2+} transients as well. A slow rise in diastolic Ca^{2+} concentration is noticeable between the early and delayed phases of repetitive Ca^{2+} transients. After release of SACs-activation, the frequency of Ca^{2+} transients was abruptly reduced, however, the amplitude of them was relatively unaffected. The diastolic Ca^{2+} concentration was still higher compared with that before activation of SACs. The activation of SACs also affected the intracellular Na^+ and K^+ concentrations. As shown in Fig. 1D, the Na^+ showed a slow rise in the intracellular concentrations, whereas K^+ (data not shown) showed a slow decrease during the activation of SACs. The release of SACs-activation slowly restored the concentration of both ions to the control level before the activation of SACs.

Role of I_{Na} in the stretch-induced automaticity

The repetitive firing of APs was found to be partly dependent on the relative conductance of voltage-gated Na^+ channel to the control (Fig. 2). Under the condition of 40%-conductance of Na^+ channel relative to the control, activation of SACs induced a transient firing of APs only and

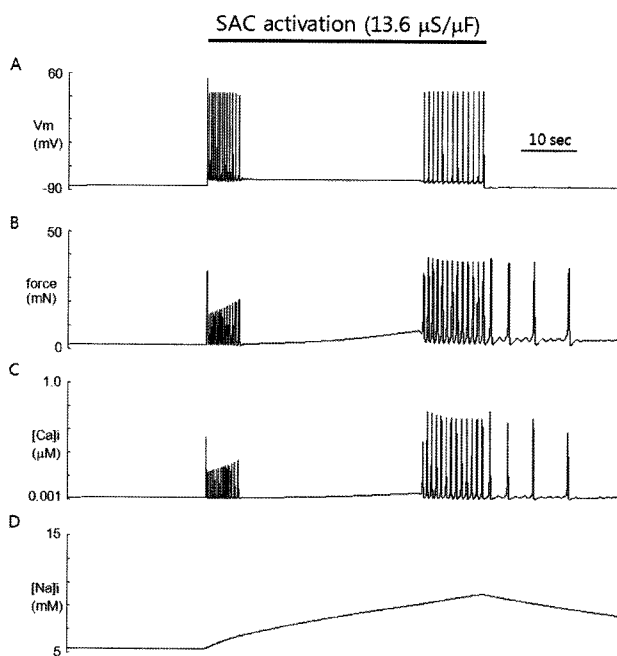


Fig. 1. Simulation of SACs-induced automaticity in the heart. Increasing SACs conductance ($13.6 \mu\text{S}/\mu\text{F}$) triggered repetitive firing of action potentials (APs) in otherwise quiescent model cell of rat atrial myocytes. The AP train is composed of early and delayed phases with different frequency (2.8 Hz vs 1.2 Hz). Upon releasing the SACs activation, the model cell stopped firing, leaving very small depolarizations (A). Contractile force (B) and Ca^{2+} (C) show time course similar to that of membrane potential during the SACs activation. After release of SACs activation, however, the contractile force and Ca^{2+} continue oscillation with decreasing frequency. Na^+ (D) is slowly accumulated with activation of SACs and decreased slowly on release of activation.

failed to generate the repetitive firing of APs as shown in the control. As the relative conductance of Na^+ channel was increased to 60% of the control, activation of SACs still failed to generate the repetitive firing of APs in the early phase, however, eventually generated a train of APs in the delayed phase. Raising the relative conductance of Na^+ channel (80%, 100%, and 120%) gradually increased the length of APs train in both the early and delayed phases in SACs-activation period. Under the condition of 140%-conductance of Na^+ channel relative to the control, the early and delayed phases of APs merged. It is evident that the conductance of Na^+ channel determines whether the activation of SACs can induce the early phase of APs train or not. As for the delayed phase of APs train, it seems that the intracellular Na^+ -accumulation above certain level ($>15 \text{ mM}$) is responsible for its generation. The $[\text{Na}^+]_i$ -dependence of delayed phase of APs reminds us of a study (Noble and Noble, 2006) which reproduced the Na^+ -overloaded condition-induced spontaneous APs. In their study, the repetitive firing of APs was induced by calcium oscillation-driven inward surge of $\text{Na}^+/\text{Ca}^{2+}$ exchange current.

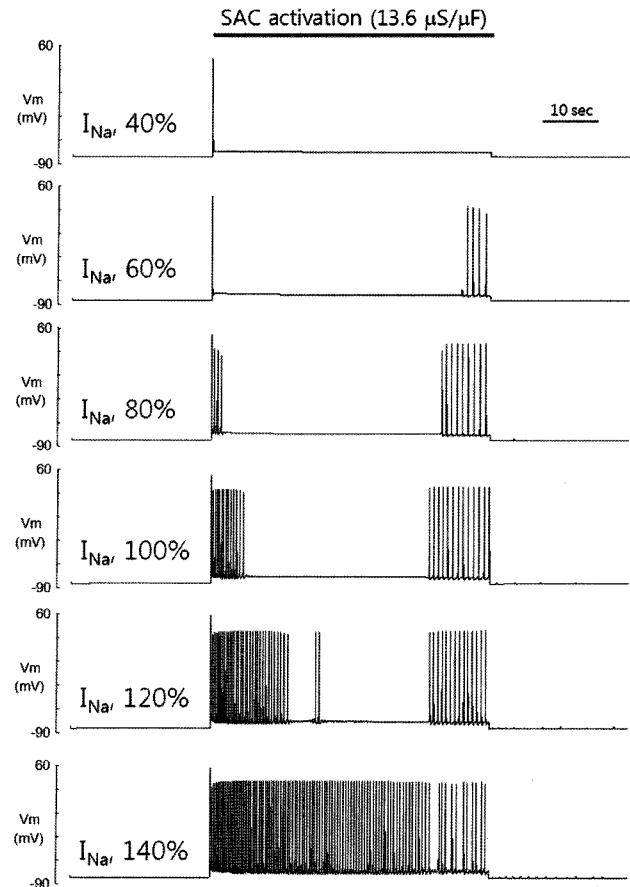


Fig. 2. Role of I_{Na} in the SACs-induced automaticity. The length of early phase in the repetitive firing of APs is dependent on the maximal conductance of voltage-gated Na^+ channel. Reducing the maximal conductance to 40% of control failed to generate the repetitive firing of APs. As the maximal conductance of voltage-gated Na^+ channel was more increased, however, the automaticity appeared and the length of early phase in repetitive firing of APs was increased. The length of delayed phase was relatively unaffected when the maximal conductance was varied between 80% and 120% relative to the control. When the maximal conductance was increased to 140% relative to the control, two phases merged together.

Role of $\text{Na}^+/\text{Ca}^{2+}$ exchange current in the stretch-induced automaticity

In order to investigate whether the $\text{Na}^+/\text{Ca}^{2+}$ exchange current (I_{NaCa}) drives the second phase of APs train during the SACs-activation (Youm et al, 2006), the amplitude of I_{NaCa} was clamped before the second phase of APs train appeared. As shown in Fig. 3A, the activation of SACs in the mathematical model of rat atrial myocytes without electrical pacing induced the early phase of APs train only. The second phase of APs train was not induced. Meanwhile, the intracellular changes in $[\text{Na}^+]_i$, $[\text{Ca}^{2+}]_i$, and contractile force were the same as those by control (without I_{NaCa} clamp). The uncoupling of excitation and contraction by I_{NaCa} clamp indicates that the I_{NaCa} couples the intracellular changes in $[\text{Ca}]_i$ to the spontaneous firing of APs in the delayed phase of APs train. The reverse-mode operation of

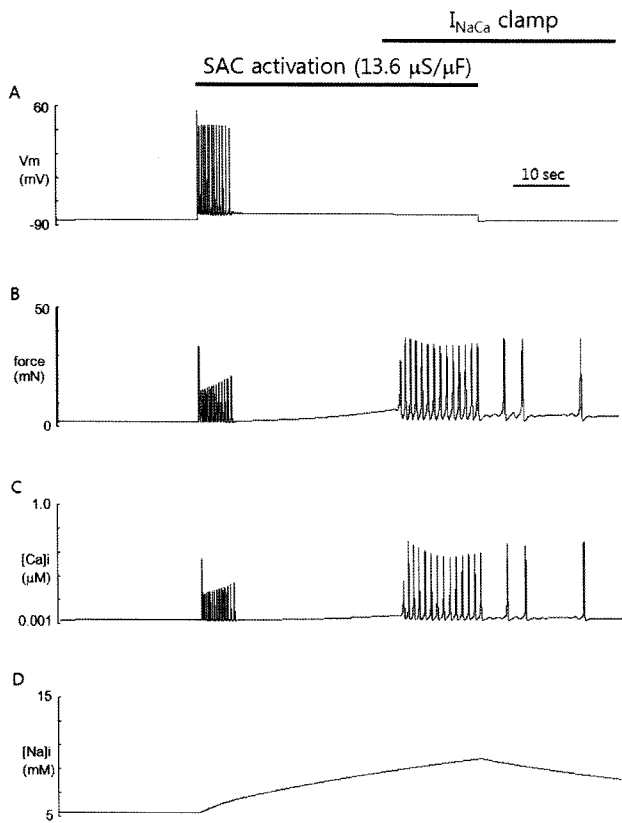


Fig. 3. Role of I_{NaCa} in SACs-induced automaticity. Clamping of I_{NaCa} just before the delayed phase of repetitive firing of APs by SACs activation abolished the delayed phase, leaving oscillations of contractile force and Ca^{2+} unaffected. Time course of $[Na^+]_i$ was also unaffected compared with that of the control (see Fig. 1D).

I_{NaCa} induced by Ca^{2+} transients is supposed to drive the initial depolarization, which subsequently activates I_{Na} , thus causing action potential firing. The Na^+ -accumulation and the resultant increase in $[Ca^{2+}]_i$ during the prolonged activation of SACs seem to be responsible for the calcium-induced calcium release, reflected by Ca^{2+} transients.

Role of intracellular ions in the stretch-induced automaticity

The ion concentrations ($[Na^+]_i$, $[K^+]_i$, and $[Ca^{2+}]_i$) were clamped during the activation of SACs in order to see whether the mathematical model could still induce persistent APs train without intracellular ionic changes or not. As shown in Fig. 4C, the APs train was persistent during the activation of SACs, indicating that the early phase of APs train can be induced by purely electrical means. However, the reduction in the relative conductance of voltage-gated Na^+ channel reduced the length of early phase of APs train with no later APs train (Fig. 4B). Therefore, it could be concluded that the length of the early phase of APs train is dependent on the conductance of voltage-gated Na^+ channel, and that the delayed phase of APs train is dependent on the gradual accumulation of Na^+ and Ca^{2+} . The longer duration of early phase of automaticity with ion clamp condition (Fig. 4C) compared to that without

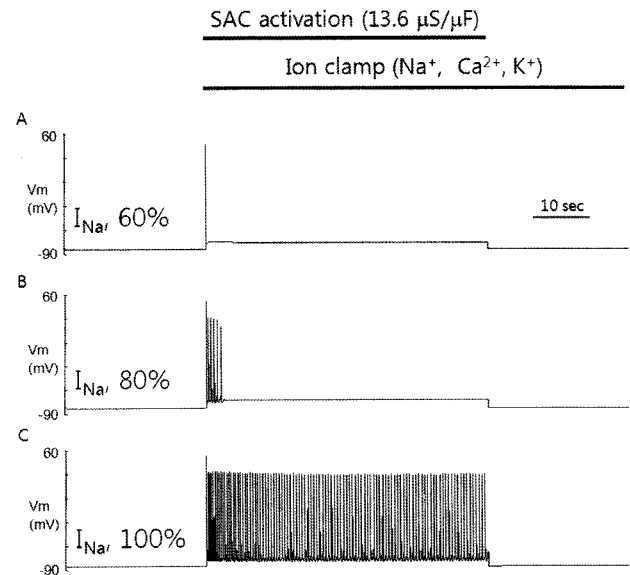


Fig. 4. Role of intracellular cations in the SACs-induced automaticity. Clamping of cation concentrations during the SACs activation abolished the delayed phase of SACs-induced automaticity, leaving only the early phase under conditions of 60% (A) and 80% (B) in maximal conductance of voltage-gated Na^+ channel relative to the control. The firing of APs continued during the SACs activation under the condition of 100% (C) in maximal conductance relative to the control, indicating that the early phase is driven by purely electrical means.

ion clamp condition suggests that the stretch-dependent changes in ion concentration are against the early phase of automaticity.

DISCUSSION

The objectives of this study were to reproduce the repetitive firing of spontaneous APs induced by mechanical stretch and to investigate which mechanism is involved in the phenomenon by exploiting our mathematical model of rat atrial myocytes. The model simulation could reproduce the automaticity by mechanical stretch. The time lapse of the automaticity could be divided into two phases: the early and delayed phases. The simulation results suggest that the early phase is mainly driven by increased background conductance of voltage-gated Na^+ channel with stretch-induced depolarization. The delayed phase is considered to be driven by the reverse-mode operation of Na^+/Ca^{2+} exchange current secondary to the accumulation of Na^+ and Ca^{2+} through SACs. The induced automaticity by stretch in quiescent atrial cells may act as a focus to initiate and maintain AF in concert with other arrhythmogenic changes in the heart.

Role of I_{Na} in the automaticity induced by stretch

One unexpected finding in this computational study is that the conductance of voltage-gated fast Na^+ channel determines the initiation and duration of the repetitive firing of APs which are induced by stretch, irrespective of intracellular accumulation of cations such as Na^+ and Ca^{2+} . There have been reports that the fast Na^+ channel but not

Ca^{2+} channel plays a significant role in the spontaneously occurring electrical activity of the embryonic or newborn heart (Prakash et al, 1996; Baruscotti et al, 2000). The involvement of I_{Na} in the pacemaker activity has also been demonstrated in the adult heart (Maier et al, 2003; Lei et al, 2004). It might be hypothesized that the I_{Na} could play a significant role in the pacemaker activity, especially if the resting membrane potential is shifted to the positive direction enough to induce window current through fast Na^+ channel. In the present study, the activation of SACs seems to take the role of shifting the resting membrane potential to the positive direction, thereby augmenting the amplitude of I_{Na} . The idea that I_{Na} can contribute to diastolic depolarization was demonstrated in canine cardiac Purkinje cells. The spontaneous discharge in Purkinje cells was suppressed by tetrodotoxin (TTX), implicating that the last part of diastolic depolarization is driven by a TTX-sensitive component (Vassalle and Scidá, 1979; Rota and Vassalle, 2003). Rota and Vassalle (2003) concluded that a voltage- and time-dependent inward Na^+ current with slow inactivation kinetics plays a significant role in the initiation and maintenance of spontaneous discharge in Purkinje cells. The mathematical model of I_{Na} used in the present study also includes ultra-slow inactivation separately from the 4-state model (Nuss et al, 1996; Matsuoka et al, 2003). Taken together, the kinetics and amplitude of I_{Na} are believed to determine whether a cardiac myocyte could show an early phase of automaticity in response to mechanical stretch.

Role of I_{NaCa} in the automaticity induced by stretch

Recently, rhythmic intracellular Ca^{2+} cycling has been proposed as one of integral components of biological clock which drives a pacemaker depolarization of sinoatrial nodal pacemaker cells (SANs) (Sanders et al, 2006). The local spontaneous releases of Ca^{2+} through ryanodine receptors (RyRs) in concert with ion channel clock have been suggested to activate sufficient amplitude of I_{NaCa} to initiate or modulate diastolic depolarization (Vinogradova et al, 2005; Maltsev and Lakatta, 2008). A computational study using a Purkinje fiber model reproduced a repetitive firing of APs in a condition of Na^+ and Ca^{2+} overload (Noble, 2002). The basis of induced automaticity is the Ca^{2+} oscillation triggered by Na^+ and Ca^{2+} overload and subsequent oscillatory activation of I_{NaCa} . Ca^{2+} oscillation, and arrhythmia was identified in rat ventricular myocytes, which were Na^+ -loaded by strophanthidin which is known as a selective inhibitor of Na^+/K^+ ATPase (Satoh et al, 2003). Recently, we proposed that SACs gradually increase the amplitude of Ca^{2+} transients via a reverse-mode operation of the $\text{Na}^+/\text{Ca}^{2+}$ exchanger which could be activated by intracellular Na^+ loading through SACs in response to stretch (Youm et al, 2006). The intracellular Na^+ loading in response to stretch was identified in mouse ventricular myocytes, showing about two-fold increase in $[\text{Na}^+]_i$ by 3 μm of stretch for 2 min (Isenberg et al, 2003). Our present study also reproduced the Ca^{2+} oscillation by Na^+ overload and subsequent activation of I_{NaCa} , causing delayed automaticity in response to stretch (Fig. 1A). Taken together, it could be hypothesized that the stretch could induce delayed automaticity when Na^+ influx through SACs reaches a threshold to trigger Ca^{2+} oscillation. The threshold level of $[\text{Na}^+]_i$ which induces Ca^{2+} oscillation was around 15 mM in our computational study and 14 mM in the study by

Noble and Noble (2006). The brief period of Ca^{2+} oscillation and contraction after release of stretch (Fig. 1B, C) could be attributed to the slow recovery of $[\text{Na}^+]_i$. The AP, however, stopped firing after release of stretch, because the activation of I_{NaCa} alone is not enough to make the membrane potential reach the threshold of I_{Na} activation.

Clinical implications of this study

The AF-inducibility of SACs was identified in perfused rabbit hearts, where the AF initiated by dilating atria was successfully inhibited by blocking SACs with a specific peptide in the venom of the tarantula *Grammostola spatulata* (Bode et al, 2001). The basic mechanism of how SACs are involved in the arrhythmogenesis has not yet been presented. There is an evidence to show that AF in human atrial myocytes is associated with increased spontaneous Ca^{2+} release from the sarcoplasmic reticulum (Hove-Madsen et al, 2004). The spontaneously occurring Ca^{2+} transients are expected to induce transient afterdepolarizations or abnormal automaticity in the atria. The abnormal automaticity (Mary-Rabine et al, 1983) and triggered activity (Hordof et al, 1978) have been proposed as major mechanisms causing atrial arrhythmias. The abnormal automaticity was suggested to induce arrhythmias by causing conduction disturbances or even conduction block in advanced stage (Ferrier, 1977). Considering that the common event causing arrhythmias in the Na^+ overloaded and dilated heart is increased activation of I_{NaCa} , the I_{NaCa} blocker, especially for the Ca^{2+} influx mode, may have therapeutic potential against the stretch-induced AF (Satoh et al, 2003).

Limitations of this study

A limitation of this study is that only cation non-selective SACs was incorporated into the mathematical model of SACs. The stretch-sensitive TREK (Terrenoire et al, 2001; Niu and Sachs, 2003; Youm, 2003) and swelling activated Cl^- -selective channels (Sorota, 1992; Tseng, 1992; Baumgarten et al, 2003) were not considered. Even though they are all activated by stretch, the mode of stretch appears to determine their selective activation. It has been proposed that mechanical stretch along the longitudinal axis of a cell activates only the cation non-selective SACs, whereas the tension developed by membrane expansion could activate K^+ - and Cl^- -selective SACs as well as cation non-selective SACs (Zhang et al, 2000; Youm, 2003). The reversal potential of SACs activated by mechanical stretch under a physiological condition was -6.1 mV, implying that the stretch-activated currents are mostly cation non-selective (Zhang et al, 2000). In order to reproduce and predict the effects of membrane expansion, however, the incorporation of K^+ - and Cl^- -selective SACs are also mandatory. SACs have also been known to be linked to intracellular signalling mechanisms, including phospholipases, tyrosin kinases, mitogen-activated protein kinases, etc. (Vandenburgh, 1992; Sadoshima and Izumo, 1993). Since little is known as yet about the reaction kinetics related to the intracellular signalling events, we did not incorporate them into the mathematical model of rat atrial myocytes.

Furthermore, we did not consider the time-dependent behaviour of SAC (Hu and Sachs, 1996; Zhang et al, 2000). We assumed that the increase in SACs conductance is statically active during the period of stretch. In the real experiment, however, the activation of SACs showed growth and

decay during sustained stretch (>1 min). Formulation of complex membrane dynamics including the effects of a deformational force on the cell membrane should be incorporated into the mathematical model to reproduce and predict time course of stretch-induced changes in cellular activity.

Conclusions

The cation non-selective SACs contribute to the stretch-induced automaticity. The primary stretch-induced firing of APs is purely driven by electrical means, and the length of APs train is dependent on the maximal conductance of voltage-gated Na^+ channel. The gradual Na^+ loading by SACs activates the operation of reverse mode $\text{Na}^+/\text{Ca}^{2+}$ exchanger, increasing the amplitude of Ca^{2+} transients during sustained stretch. The delayed firing of APs is driven by this reverse-mode operation of $\text{Na}^+/\text{Ca}^{2+}$ exchange current. The SAC might contribute to the generation of cardiac arrhythmias, such as atrial tachycardia and AF, by enhancing automaticity in quiescent atrial myocytes.

ACKNOWLEDGEMENT

This work was supported by Korea Research Foundation Grant funded by Korea Government (MOEHRD, Basic Research Promotion Fund) (KRF-2005-003-E00014) and the 2004 Inje University research grant.

REFERENCES

- Baruscotti M, DiFrancesco D, Robinson RB. Na^+ current contribution to the diastolic depolarization in newborn rabbit SA node cells. *Am J Physiol* 279: H2303–H2309, 2000
- Baumgarten CM, Clemo HF. Swelling-activated chloride channels in cardiac physiology and pathophysiology. *Prog Biophys Mol Biol* 82: 25–42, 2003
- Bode F, Katchman A, Woosley RL, Franz MR. Gadolinium decreases stretch-induced vulnerability to atrial fibrillation. *Circulation* 101: 2200–2205, 2000
- Bode F, Sachs F, Franz MR. Tarantula peptide inhibits atrial fibrillation. *Nature* 409: 35–36, 2001
- Boland J, Troquet J. Intracellular action potential changes induced in both ventricles of the rat by an acute right ventricular pressure overload. *Cardiovasc Res* 14: 735–740, 1980
- Boyle WA, Nerbonne JM. Two functionally distinct 4-aminopyridine-sensitive outward K^+ currents in rat atrial myocytes. *J Gen Physiol* 100: 1041–1067, 1992
- Bustamante JO, Ruknudin A, Sachs F. Stretch-activated channels in heart cells: relevance to cardiac hypertrophy. *J Cardiovasc Pharmacol* 17: S110–S113, 1991
- Craelius W. Stretch-activation of rat cardiac myocytes. *Exp Physiol* 78: 411–423, 1993
- Dean JW, Lab MJ. Arrhythmia in heart failure: role of mechanically induced changes in electrophysiology. *Lancet* 1: 1309–1312, 1989
- Ferrier GR. Digitalis arrhythmias: role of oscillatory afterpotentials. *Prog Cardiovasc Dis* 19: 459–474, 1977
- Franz MR, Bode F. Mechano-electrical feedback underlying arrhythmias: the atrial fibrillation case. *Prog Biophys Mol Biol* 82: 163–174, 2003
- Franz MR, Burkhoff D, Yue DT, Sagawa K. Mechanically induced action potential changes and arrhythmia in isolated and in situ canine hearts. *Cardiovasc Res* 23: 213–223, 1989
- Franz MR, Cima R, Wang D, Profitt D, Kurz R. Electrophysiological effects of myocardial stretch and mechanical determinants of stretch-activated arrhythmias [published erratum appears in *Circulation* 1992;86:1663]. *Circulation* 86: 968–978, 1992
- Hansen DE. Mechano-electrical feedback effects of altering preload, afterload, and ventricular shortening. *Am J Physiol* 264: H423–H432, 1993
- Hordof AJ, Spotnitz A, Mary-Rabine L, Edie RN, Rosen MR. The cellular electrophysiologic effects of digitalis on human atrial fibers. *Circulation* 57: 223–229, 1978
- Hove-Madsen L, Llach A, Bayes-Genis A, Roura S, Rodriguez Font E, Aris A, Cinca J. Atrial fibrillation is associated with increased spontaneous calcium release from the sarcoplasmic reticulum in human atrial myocytes. *Circulation* 110: 1358–1363, 2004
- Hoyer J, Distler A, Haase W, Gögelein H. Ca^{2+} influx through stretch-activated cation channels activates maxi K^+ channels in porcine endocardial endothelium. *Proc Natl Acad Sci USA* 91: 2367–2371
- Hu H, Sachs F. Mechanically activated currents in chick heart cells. *J Membr Biol* 154: 205–216, 1996
- Isenberg G, Kazanski V, Kondratev D, Gallitelli MF, Kiseleva I, Kamkin A. Differential effects of stretch and compression on membrane currents and $[\text{Na}^+]_i$ in ventricular myocytes. *Prog Biophys Mol Biol* 82: 43–56, 2003
- Kaufmann R, Theophile U. Automatiiefördernde Dehnungseffekte an Purkinje-Fäden, Papillarmuskeln und Vorhoftrabekeln von Rhesus-Affen. *Pflügers Arch* 297: 174–189, 1967
- Kiseleva I, Kamkin A, Wagner KD, Theres H, Ladhoff A, Scholz H, Günther J, Lab MJ. Mechano-electric feedback after left ventricular infarction in rats. *Cardiovasc Res* 45: 370–378, 2000
- Lab MJ. Mechanically dependent changes in action potentials recorded from the intact frog ventricle. *Circ Res* 42: 519–528, 1978
- Lei M, Jones SA, Liu J, Lancaster MK, Fung SS, Dobrzynski H, Camelliti P, Maier SK, Noble D, Boyett MR. Requirement of neuronal- and cardiac-type sodium channels for murine sinoatrial node pacemaking. *J Physiol* 559: 835–848, 2004
- Maier SK, Westenbroek RE, Yamanushi TT, Dobrzynski H, Boyett MR, Catterall WA, Scheuer T. An unexpected requirement for brain-type sodium channels for control of heart rate in the mouse sinoatrial node. *Proc Natl Acad Sci USA* 100: 3507–3512, 2003
- Maltsev VA, Lakatta EG. Dynamic interactions of an intracellular Ca^{2+} clock and membrane ion channel clock underlie robust initiation and regulation of cardiac pacemaker function. *Cardiovasc Res* 77: 274–284, 2008
- Mary-Rabine L, Albert A, Pham TD, Hordof A, Fenoglio JJ Jr, Malm JR, Rosen MR. The relationship of human atrial cellular electrophysiology to clinical function and ultrastructure. *Circ Res* 52: 188–199, 1983
- Matsuoka S, Sarai N, Kuratomi S, Ono K, Noma A. Role of individual ionic current systems in ventricular cells hypothesized by a model study. *Jpn J Physiol* 53: 105–123, 2003
- Niu W, Sachs F. Dynamic properties of stretch-activated K^+ channels in adult rat atrial myocytes. *Prog Biophys Mol Biol* 82: 121–135, 2003
- Noble D. Simulation of Na/Ca exchange activity during ischemia. *Ann N Y Acad Sci* 976: 431–437, 2002
- Noble D, Noble PJ. Late sodium current in the pathophysiology of cardiovascular disease: consequences of sodium-calcium overload. *Heart* 92: iv1–iv5, 2006
- Nuss HB, Balsler JR, Orias DW, Lawrence JH, Tomaselli GF, Marban E. Coupling between fast and slow inactivation revealed by analysis of a point mutation (F1304Q) in μl rat skeletal muscle sodium channels. *J Physiol* 494: 411–429, 1996
- Prakash P, Meera P, Tripathi O. Effects of calcium channel blockers on spontaneous electrical activity of freshly isolated three-day-old embryonic chick ventricle. *Reprod Fertil Dev* 8: 921–929, 1996
- Psaty BM, Manolio TA, Kuller LH, Kronmal RA, Cushman M, Fried LP, White R, Furberg CD, Rautaharju PM. Incidence of and risk factors for atrial fibrillation in older adults. *Circulation* 96: 2455–2461, 1997
- Rota M, Vassalle M. Patch-clamp analysis in canine cardiac

- Purkinje cells of a novel sodium component in the pacemaker range. *J Physiol* 548: 147–165, 2003
- Sadoshima J, Izumo S. Mechanical stretch rapidly activates multiple signal transduction pathways in cardiac myocytes: potential involvement of an autocrine/paracrine mechanism. *EMBO J* 12: 1681–1692, 1993
- Sanders L, Rakovic S, Lowe M, Mattick PA, Terrar DA. Fundamental importance of Na^+ - Ca^{2+} exchange for the pacemaking mechanism in guinea-pig sino-atrial node. *J Physiol* 571: 639–649, 2006
- Sarai N, Matsuoka S, Kuratomi S, Ono K, Noma A. Role of individual ionic current systems in the SA node hypothesized by a model study. *Jpn J Physiol* 53: 125–134, 2003
- Satoh H, Mukai M, Urushida T, Katoh H, Terada H, Hayashi H. Importance of Ca^{2+} influx by Na^+ / Ca^{2+} exchange under normal and sodium-loaded conditions in mammalian ventricles. *Mol Cell Biochem* 242: 11–17, 2003
- Sorota S. Swelling-induced chloride-sensitive current in canine atrial cells revealed by whole-cell patch-clamp method. *Circ Res* 70: 679–687, 1992
- Taggart P. Mechano-electric feedback in the human heart. *Cardiovasc Res* 32: 38–43, 1996.
- Terrenoire C, Lauritzen I, Lesage F, Romey G, Lazdunski M. A TREK-1-like potassium channel in atrial cells inhibited by beta-adrenergic stimulation and activated by volatile anesthetics. *Circ Res* 89: 336–342, 2001
- Tseng GN. Cell swelling increases membrane conductance of canine cardiac cells: evidence for a volume-sensitive Cl channel. *Am J Physiol* 262: C1056–C1068, 1992
- Vandenburgh HH. Mechanical forces and their second messengers in stimulating cell growth in vitro. *Am J Physiol* 262: R350–R355, 1992
- Vassalle M, Scidá EE. The role of sodium in spontaneous discharge in the absence and in the presence of strophanthidin. *Fed Proc* 38: 880, 1979
- Vaziri SM, Larson MG, Benjamin EJ, Levy D. Echocardiographic predictors of nonrheumatic atrial fibrillation. The Framingham Heart Study. *Circulation* 89: 724–730, 1994
- Vinogradova TM, Maltsev VA, Bogdanov KY, Lyashkov AE, Lakatta EG. Rhythmic Ca^{2+} oscillations drive sinoatrial nodal cell pacemaker function to make the heart tick. *Ann N Y Acad Sci* 1047: 138–156, 2005
- Wagner MB, Kumar R, Joyner RW, Wang Y. Induced automaticity in isolated rat atrial cells by incorporation of a stretch-activated conductance. *Pflügers Arch* 447: 819–829, 2004
- Youm JB. Stretch-activated K^+ channels in rat atrial myocytes. *Korean J Physiol Pharmacol* 7: 341–348, 2003
- Youm JB, Han J, Kim N, Zhang YH, Kim E, Joo H, Leem CH, Kim SJ, Cha KA, Earm YE. Role of stretch-activated channels on the stretch-induced changes of rat atrial myocytes. *Prog Biophys Mol Biol* 90: 186–206, 2006
- Zhang YH, Youm JB, Sung HK, Lee SH, Ryu SY, Ho WK, Earm YE. Stretch-activated and background non-selective cation channels in rat atrial myocytes. *J Physiol* 523: 607–619, 2000